Title: Gut bacterial tyrosine decarboxylases restrict the bioavailability of levodopa, the primary treatment in Parkinson's disease

Authors: Sebastiaan P. van Kessel[1], Alexandra K. Frye[1], Ahmed O. El-Gendy[1,2], Maria Castejon[1], Ali Keshavarzian[3], Gertjan van Dijk[4], Sahar El Aidy[1*†]

Affiliations:

[1] Department of Molecular Immunology and Microbiology, Groningen Biomolecular Sciences and Biotechnology Institute (GBB), University of Groningen, Groningen, The Netherlands.

[2] Department of Microbiology and Immunology, Faculty of Pharmacy, Beni-Suef University, Beni-Suef, Egypt

[3] Division of Digestive Disease and Nutrition, Section of Gastroenterology, Department of Internal Medicine, Rush University Medical Center, Chicago, Illinois.

[4] Department of Behavioral Neuroscience, Groningen Institute for Evolutionary Life Sciences (GELIFES), University of Groningen, Groningen, The Netherlands.

[*] Corresponding author. Email: sahar.elaidy@rug.nl

[†] Present address: Groningen Biomolecular Sciences and Biotechnology Institute (GBB), University of Groningen, Nijenborg 7, 9747 AG Groningen, The Netherlands. P:+31(0)503632201.

One Sentence Summary:

L-DOPA conversion by bacterial tyrosine decarboxylase in the small intestine is a significant explanatory factor for the highly variable L-DOPA dosage regimens required in the treatment of individual Parkinson's patients.

Abstract

Human gut bacteria play a critical role in the regulation of immune and metabolic systems, as well as in the function of the nervous system. The microbiota senses its environment and responds by releasing metabolites, some of which are key regulators of human health and disease. In this study, we identify and characterize gut-associated bacteria in their ability to decarboxylate L-3,4-dihydroxyphenylalanine (L-DOPA) via the tyrosine decarboxylases, which are mainly present in the class Bacilli. Although the bacterial tyrosine decarboxylases have a higher affinity for tyrosine compared to L-DOPA, this does not affect their ability to convert L-DOPA to dopamine, nor does any inhibitor of the human decarboxylase. This study indicates that *in situ* bioavailability of L-DOPA is compromised by the gut bacterial tyrosine decarboxylase gene abundance in Parkinson's patients. Finally, we show that the tyrosine decarboxylase gene abundance in the microbiota of the site of L-DOPA absorption, the proximal small intestine, significantly influences L-DOPA bioavailability in the plasma of rats. Our results highlight the role of microbial metabolism in drug bioavailability, and that specifically, small intestinal abundance of bacterial tyrosine decarboxylase can explain the highly variable L-DOPA dosage regimens required in the treatment of individual Parkinson's patients.

Introduction

The complex communities of microbiota inhabiting the mammalian gut have a significant impact on the health of their host (*1*). Numerous reports indicate microbiota, and in particular its metabolic products, have a crucial effect on various health and diseased states. Host immune system and brain development, metabolism, behavior, stress and pain response have all been reported to be subject to microbial modulation (*2*-*6*). In addition, it is becoming increasingly clear that gut microbiota can play a detrimental role in the modulation of drug pharmacokinetics and drug bioavailability (*7*, *8*). Parkinson's disease, the second most common neurodegenerative disorder, affecting 1% of the global population over the age of 60, has recently been correlated with alterations in microbial gut composition (*9*-*12*). To date, L-DOPA (also termed levodopa) is the most effective treatment available for Parkinson's patients. In humans, peripheral L-DOPA metabolism involves DOPA decarboxylase, which converts L-DOPA to dopamine, thus preventing the passage of L-DOPA to its site of action in

the brain, as dopamine cannot pass the blood-brain barrier. For this reason, Parkinson's patients are treated with a DOPA decarboxylase inhibitor (primarily carbidopa) in combination with L-DOPA to enhance the effectiveness of L-DOPA delivery to the brain. Nonetheless, the pharmacokinetics of L-DOPA/carbidopa treatment varies significantly among patients, some are resistant to the treatment, others undergo fluctuating response towards the treatment over time, thus require increasing L-DOPA dosage regimen leading to increased severity of adverse effects like dyskinesia (*13*). What remains to be clarified is whether inter-individual variations in gut microbiota composition play a causative role in the variation of treatment efficacy.

Several amino acid decarboxylases have been annotated in bacteria. Tyrosine decarboxylase genes have especially been encoded in the genome of several bacterial species in the genera *Lactobacillus* and *Enterococcus (14, 15)* Though tyrosine decarboxylase is named for its capacity to decarboxylate L-tyrosine to produce tyramine, it might also have the ability to decarboxylate L-DOPA to produce dopamine (*15*) due to the high similarity of the chemical structures of these substrates. This implies that tyrosine decarboxylase produced by gut microbiota might interfere with L-DOPA bioavailability, which could be of clinical significance in the L-DOPA treatment of Parkinson's patients.

The aim of the present study is to parse out the effect of L-DOPA metabolizing bacteria, particularly in the proximal small intestine, where L-DOPA is absorbed. Initially, we established the tyrosine decarboxylases present in small intestinal bacteria efficiently converted L-DOPA to dopamine, confirming their capacity to modulate the *in situ* bioavailability of the primary drug used in the treatment of Parkinson's patients. We show that higher relative abundance of bacterial tyrosine decarboxylase in fecal samples of Parkinson's patients positively correlates with higher daily L-DOPA dosage requirement and duration of disease. We further confirm our findings in rats orally administered a mixture of L-DOPA/carbidopa, illustrating that L-DOPA levels in plasma negatively correlate with the abundance of bacterial tyrosine decarboxylase gene in the proximal small intestine.

Results

Proximal small intestinal bacteria convert L-DOPA to dopamine

To determine whether proximal small intestinal microbiota maintain the ability to metabolize L-DOPA, luminal samples from the jejunum of wild-type Groningen rats were incubated *in vitro* with L-DOPA and analyzed by High-Performance Liquid Chromatography with Electrochemical Detection (HPLC-ED). The chromatograms revealed that L-DOPA decarboxylation (**Fig. 1A**) coincides with the conversion of tyrosine to tyramine (**Fig. 1B-E**). In addition, no other metabolites derived from L-DOPA were detected. To support the *ex vivo* experiment results, the uptake of L-DOPA was quantified in plasma samples from specific pathogen free and germ-free female C57 BL/6J mice after oral gavage with L-DOPA. HPLC-ED analysis revealed higher levels of L-DOPA and its metabolites dopamine and DOPAC (3,4-Dihydroxyphenylacetic acid) in plasma samples of germ-free mice compared to their conventional counterparts (**Fig. S1**). Taken together, the results suggest a tyrosine decarboxylase is involved in L-DOPA metabolism by gut bacteria, which may, in turn, interfere with L-DOPA uptake in the proximal small intestine.

Tyrosine decarboxylase is responsible for L-DOPA decarboxylation

The coinciding tyrosine and L-DOPA decarboxylation observed in the luminal content of jejunum was the basis of our hypothesis that tyrosine decarboxylase is the enzyme involved in both conversions. Species of the genera *Lactobacillus* and *Enterococcus* have been reported to encode this enzyme (*14-16*). To investigate whether these genera indeed represent the main tyrosine decarboxylase encoding bacterial groups of the small intestine microbiota, the tyrosine decarboxylase protein (EOT87933) from the laboratory strain *Enterococcus faecalis* v583 was used as a query to search the US National Institutes of Health Human Microbiome Project (HMP) protein database, to identify whether other (small intestinal) gut bacteria also encode tyrosine decarboxylases. This analysis exclusively identified tyrosine decarboxylase proteins in species belonging to the Bacilli class, including more than 50 *Enterococcus* strains (mainly *E. faecium* and *E. faecalis*) and several *Lactobacillus* and *Staphylococcus* species (**Fig. S2A**). Next, we aligned the genome of *E. faecalis* v583 with two gut bacterial isolates, *E. faecium* W54, and *L. brevis* W63, illustrating the conservation of the tyrosine

decarboxylase (*tdc*)-operon among these species (**Fig. 2A**). Intriguingly, analysis of *E. faecium* genomes revealed that this species encodes a second, paralogous *tdc* gene ($^{P}TDC_{EFM}$) that did not align with the conserved *tdc*-operon and was absent from the other species (**Fig. 2A, Fig. S2A, Data file S1**).

To support our *in silico* data, a comprehensive screening of *E. faecalis* v583, *E. faecium* W54, and *L. brevis* W63 and 77 additional clinical and human isolates of *Enterococcus* was performed. All *Enterococci* isolates and *L. brevis* were able to convert tyrosine and L-DOPA into tyramine and dopamine, respectively (**Fig. 2B-D, Table S1**). Notably, our HPLC-ED analysis revealed considerable variability among the tested strains with regard to their efficiency to decarboxylate L-DOPA. *E. faecium* and *E. faecalis* were drastically more efficient at converting L-DOPA to dopamine, compared to *L. brevis*. Growing *L. brevis* in different growth medium did not change the L-DOPA decarboxylation efficacy (**Fig. S2B,C**). To eliminate the possibility that other bacterial amino acid decarboxylases is involved in L-DOPA conversion observed in the jejunal content we expanded our screening to include live bacterial species harboring PLP-dependent amino acid decarboxylases previously identified by Williams et al (*17*). None of the tested bacterial strains encoding different amino acid decarboxylases could decarboxylate L-DOPA (**Fig. S2D-G, Table S2**).

To verify that the tyrosine decarboxylase gene is solely responsible for L-DOPA decarboxylation in *Enterococcus*, wild type *E. faecalis* v583 (EFS^{WT}) was compared with a mutant strain ($EFS^{\Delta TDC}$) in which both the tyrosine decarboxylase gene (*tdcA*) and tyrosine transporter (*tyrP*) were deleted (*14*), (**Fig. 2E**). Overnight incubation of EFS^{WT} and $EFS^{\Delta TDC}$ with L-DOPA resulted in production of dopamine in the supernatant of EFS^{WT} but not $EFS^{\Delta TDC}$ (**Fig. 2F**), confirming the pivotal role of these genes in this conversion. To rule out that deletion of *tyrP* alone could explain the observed result by an impaired L-DOPA import, cell-free protein extracts were incubated with 1 mM L-DOPA overnight at 37°C. While EFS^{WT} converted all supplied L-DOPA into dopamine, no dopamine production was observed in the $EFS^{\Delta TDC}$ cell-free protein extracts (**Fig. 2G**). Collectively, results show tyrosine decarboxylase is encoded by gut bacterial species known to dominate the proximal small intestine and that this enzyme is exclusively responsible for converting L-DOPA to dopamine by these bacteria, although the efficiency of that conversion displays considerable species-dependent variability.

High levels of tyrosine do not prevent bacterial decarboxylation of L-DOPA

To test whether the availability of the primary substrate for bacterial tyrosine decarboxylases (i.e., tyrosine) could inhibit the uptake and decarboxylation of L-DOPA, the growth, metabolites, and pH (previously shown to affect the expression of tyrosine decarboxylases (*14*)) of *E. faecium* v583 and *E. faecalis* W54 were analyzed over time. 100 µM L-DOPA was added to the bacterial cultures, whereas approximately 500 µM tyrosine was present in the growth media. Remarkably, L-DOPA and tyrosine were converted simultaneously, even in the presence of these excess levels of tyrosine (1:5 L-DOPA to tyrosine), albeit at a slower conversion rate for L-DOPA (**Fig. 3A-B**). Notably, the decarboxylation reaction appeared operational throughout the exponential phase of growth for *E. faecalis*, whereas it is only observed in *E. faecium* when this bacterium entered the stationary phase of growth, suggesting differential regulation of the tyrosine decarboxylase expression in these species.

To further characterize the substrate specificity and kinetic parameters of the bacterial tyrosine decarboxylases, tyrosine decarboxylase genes from *E. faecalis* v583 (TDC_{EFS}) and *E. faecium* W54 (TDC_{EFM} and $^{P}TDC_{EFM}$) were expressed in *Escherichia coli* BL21 (DE3) and then purified. Michaelis-Menten kinetics indicated each of the studied enzymes had a significantly higher affinity (K_m) (**Fig. 3C-I**) and catalytic efficiency (K_{cat}/K_m) for tyrosine than for L-DOPA (**Table 1**). Despite the differential substrate affinity, our findings illustrate that high levels of tyrosine do not prevent the decarboxylation of L-DOPA in batch culture.

Carbidopa is a potent inhibitor for the human decarboxylase but not *bacterial* decarboxylases

To assess the extent to which human DOPA decarboxylase inhibitors could affect bacterial decarboxylases, several human DOPA decarboxylase inhibitors (carbidopa, benserazide, and methyldopa) were tested on purified bacterial tyrosine decarboxylase and on the corresponding bacterial batch cultures carrying the gene. Comparison of the given inhibitory constants (K_i^{TDC}/K_i^{DDC}) demonstrates carbidopa to be a 1.4-1.9 x 10^4 times more potent inhibitor of human DOPA decarboxylase than bacterial tyrosine decarboxylases (**Fig. 4A, Fig. S3; Table S3**). This is best illustrated by the observation that L-DOPA conversion by *E. faecium* W54 and *E. faecalis* v583 batch cultures (OD_{600}= ~2.0) was unaffected by co-incubation with carbidopa (equimolar or 4-fold carbidopa

relative to L-DOPA) (**Fig. 4B-C**, **S4A**). Analogously, benserazide and methyldopa did not inhibit the L-DOPA decarboxylation activity in *E. faecalis* or *E. faecium* (**Fig. S4B-C**).

These findings demonstrate the commonly applied inhibitors of human DOPA decarboxylase in L-DOPA combination therapy do not inhibit bacterial tyrosine decarboxylase dependent L-DOPA conversion, implying L-DOPA/carbidopa combination therapy for Parkinson's patients would not affect the metabolism of L-DOPA by *in situ* bacteria.

L-DOPA dosage regimen correlate with tyrosine decarboxylase gene abundance in Parkinson's patients

To determine whether the considerable variation in L-DOPA dosage required for individual Parkinson's patients could be attributed to the abundance of tyrosine decarboxylase genes in the gut microbiota, fecal samples were collected from male and female Parkinson's patients (**Table S4**) on different doses of L-DOPA/carbidopa treatment (ranging from 300 up to 1100 mg L-DOPA per day). Tyrosine decarboxylase gene-specific primers were used to quantify its relative abundance within the gut microbiota by qPCR (**Fig. S5**). Remarkably, Pearson *r* correlation analyses showed a strong positive correlation ($r = 0.70$, $R^2 = 0.49$, *p value* = 0.024) between bacterial tyrosine decarboxylase relative abundance and L-DOPA treatment dose (**Fig. 5A**), as well as with the duration of disease (**Fig. 5B**). At this stage, it is unclear whether the relative abundance of tyrosine decarboxylase in fecal samples is a reflection of its abundance in the small intestinal microbiota. This is of particular importance because L-DOPA is absorbed in proximal small intestine, and reduction in its bioavailability by bacterial tyrosine decarboxylase activity in the context of Parkinson's patients' medication regimens would only be relevant in that intestinal region. Still, the selective prevalence of tyrosine decarboxylase encoding genes in signature microbes of the small intestine microbiota supports the idea that obtained results from fecal samples are a valid representation of tyrosine decarboxylase in the small intestinal microbiota. Moreover, the significant relatedness of the relative abundance of tyrosine decarboxylase in the fecal microbiota and the required L-DOPA dosage as well as disease duration strongly supports a role for bacterial tyrosine decarboxylase in L-DOPA bioavailability.

Tyrosine decarboxylase-gene abundance in small intestine correlates with L-DOPA bioavailability in rats

To further consolidate the concept that tyrosine decarboxylase abundance in proximal small intestinal microbiota affects peripheral levels of L-DOPA in blood and dopamine/L-DOPA ratio in the jejunal luminal content, male wild-type Groningen rats (n=25) rats were orally administered 15 mg L-DOPA/3.75 mg carbidopa per kg of body weight and sacrificed after 15 minutes (point of maximal L-DOPA bioavailability in rats (*18*)). Plasma levels of L-DOPA and its metabolites dopamine and DOPAC were measured by HPLC-ED, while relative abundance of the tyrosine decarboxylase gene within the small intestinal microbiota was quantified by gene-specific qPCR (**Fig. S5**). Strikingly, Pearson *r* correlation analyses showed that the ratio between dopamine and L-DOPA levels in the proximal jejunal content positively correlated with tyrosine decarboxylase gene abundance (r= 0.78, R^2= 0.61, *P* value = 0.0001) (**Fig. 6A**), whereas the absolute L-DOPA concentration in the proximal jejunal content was negatively correlated with the abundance of the gene (r= −0.68, R^2= 0.46, *P* value = 0.0021) (**Fig. 6B**). Moreover, plasma levels of L-DOPA displayed a strong negative correlation (r = −0.66, R^2 = 0.434, *P* value = 0.004) with the relative abundance of the tyrosine decarboxylase gene (**Fig. 6C**). Findings indicate L-DOPA uptake by the host is compromised by higher abundance of gut bacterial tyrosine decarboxylase genes in the upper region of the small intestine.

Discussion

Our observation of small intestinal microbiota able to convert L-DOPA to dopamine (**Fig. 1**) was the basis of investigating the role of L-DOPA metabolizing bacteria in the context of the disparity in effective long-established L-DOPA treatment between Parkinson's patients (**Fig. 5**) for which an appropriate explanation is lacking (*19*). This study identifies a novel factor to consider in both the evaluation and treatment efficacy of L-DOPA/carbidopa pharmacokinetics and pharmacodynamics. Our primary outcome is that L-DOPA decarboxylation by gut bacteria, particularly if found in higher abundances *in vivo* in the proximal small intestine, would drastically reduce the bioavailability of L-DOPA in the body, and thereby contribute to the observed higher dosages required in some patients. Previously, reduced L-DOPA availability has been associated with *Helicobacter pylori* positive Parkinson's patients, which was explained by the observation that *H. pylori* could bind L-DOPA *in*

vitro via surface adhesins (*8*). However, this explanation is valid only for small populations within the Parkinson's patients, who suffer from stomach ulcers and thus have high abundance of *H. pylori.* Parkinson's patients also often suffer from impaired small intestinal motility (*20*), and are frequently administered proton pump inhibitors (PPIs) (*21*), leading to small intestinal bacterial overgrowth (*22, 23*). Members of Bacilli, including the genera *Enterococcus* and *Lactobacillus*, were previously identified as the predominant residents of the small intestine (*24, 25*), and in particular, *Enterococcus* has been reported to dominate in proton pump inhibitors' induced small intestinal bacterial overgrowth (*26*). These factors contribute to a higher abundance of tyrosine decarboxylase in the small intestinal microbiota, which would reduce the bioavailability of L-DOPA. Moreover, the corresponding rising levels of dopamine may further aggravate the reduced gut motility as previously shown (*27*), thereby enhancing a state of small intestinal bacterial overgrowth, and perpetuating a vicious circle leading to higher L-DOPA dosage requirement for effective treatment of individual Parkinson's patients (**Fig. 7**). Alternatively, prolonged L-DOPA administration may influence tyrosine decarboxylase-gene abundance by selectively stimulating tyrosine decarboxylase harboring bacteria in the gut. In fact, it has been shown that the fitness of *E. faecalis* v583 in low pH depends on the tyrosine decarboxylase-operon (*14*), indicating long-term exposure to L-DOPA could contribute to selection for overgrowth of tyrosine decarboxylase bacteria *in vivo* as supported by the positive correlation with disease duration and tyrosine decarboxylase-gene abundance (**Fig. 5B**). This would explain the fluctuating response to L-DOPA during prolonged disease treatment, and the consequent increased L-DOPA dosage regimen leading to increased severity of its adverse effects such as dyskinesia (*28*).

While our further investigation into the kinetics of both bacterial and human decarboxylases support the effectiveness of carbidopa to inhibit the human DOPA decarboxylase, it also shows that the same drug fails to inhibit L-DOPA bacterial tyrosine decarboxylase (**Fig. 4, S4**). This suggests a better equilibration of L-DOPA treatment between patients could potentially be achieved by co-administration of an effective inhibitor of bacterial tyrosine decarboxylase activity. To further explore this possibility, we are currently evaluating selectively suppressing growth and survival of tyrosine decarboxylase harboring bacteria *in situ* using antibiotic treatment targeted towards tyrosine decarboxylase inhibition. Alternatively, regulation of tyrosine decarboxylase gene expression, for

example by dietary intervention, could help avoid the need for high L-DOPA dosing, thus minimizing its adverse side effects.

Notably, specific strains of some of the bacterial species shown to encode and express tyrosine decarboxylases are marked as probiotics, implying that special care should be taken if certain subsets of the human population (e.g. Parkinson's patients) are given these probiotic supplementations.

Collectively, L-DOPA conversion by bacterial tyrosine decarboxylase in the small intestine is a significant explanatory factor for the highly variable L-DOPA dosage regimens required in the treatment of individual Parkinson's patients. These bacteria or their encoded tyrosine decarboxylase gene may potentially serve as a predictive biomarker for patient stratification to predict the effective L-DOPA dosage regimens for Parkinson's patients on an individual basis. Such biomarker potential is supported by the significant and robust (r=0.70) correlation observed between the relative abundance of tyrosine decarboxylase encoding bacterial genes and number of L-DOPA tablets required to treat individual Parkinson's patients (**Fig. 5A**).

A limitation of the present study is the relatively small number of patient fecal samples analyzed, and the lack of evidence as to whether high abundance of tyrosine decarboxylase *in vivo* is a cause and/or effect of higher L-DOPA dosage requirement during prolonged disease treatment. To overcome these limitations, a large longitudinal cohort of *de novo* Parkinson's patients should be designed and followed over long periods of time, with tyrosine decarboxylase gene abundance employed as a personal microbiota-based biomarker to predict individual L-DOPA dosage requirement.

Material and Methods

Study design

The study objective was to investigate the interference of small-intestine bacteria on the primary treatment of Parkinson's disease, L-DOPA. I*n vitro* experiments were employed to determine the capacity of live bacteria from the proximal small intestine to decarboxylate L-DOPA. Further, to investigate whether natural variation of tyrosine decarboxylase relative abundance in the gut could interfere with L-DOPA uptake and decarboxylation, human fecal samples from Parkinson's patients on varying doses of L-DOPA/carbidopa, and jejunal content samples from rats on oral L-DOPA/carbidopa administration, were employed and tyrosine decarboxylase levels were detected in

an unblinded manner. L-DOPA and dopamine levels quantified from jejunal luminal content were normalized to carbidopa levels detected *in vivo* to correct for intake. All data were ranked from low to high by tyrosine decarboxylase level and linear regression was performed with automatic outlier detection using the ROUT method in Graphpad Prism 7. Two significant (Q=1%) outliers (an extreme low and high point) from the total group were removed. All animal procedures were approved by the Groningen University Committee of Animal experiments (approval number: AVD1050020184844), and were performed in adherence to the NIH Guide for the Care and Use of Laboratory Animals. All replicates and statistical methods are described in the figure legends.

Bacterial growth conditions

Escherichia coli DH5a or BL21 were routinely grown aerobically in Luria-Broth (LB) at 37°C degrees with continuous agitation. Other strains listed in **Table S5** were grown anaerobically (10% H_2, 10% CO_2, 80% N_2) in a Don Whitley Scientific DG250 Workstation (LA Biosystems, Waalwijk, The Netherlands) at 37°C in an enriched beef broth based on SHIME medium (*29*) (**Table S6**). Bacteria were inoculated from −80°C stocks and grown overnight. Before the experiment, cultures were diluted 1:100 in fresh medium from overnight cultures. L-DOPA (D9628, Sigma), carbidopa (C1335, Sigma), benserazide (B7283, Sigma), or methyldopa (857416, Sigma) were supplemented during the lag or stationary phase depending on the experiment. Growth was followed by measuring the optical density (OD) at 600 nM in a spectrophotometer (UV1600PC, VWR International, Leuven, Belgium).

Cloning and heterologous expression

The human DOPA decarboxylase was ordered in pET15b from GenScript (Piscataway, USA) (**Table S5**). Tyrosine decarboxylase-encoding genes from *E. faecalis* v583 (TDC_{EFS}, accession: EOT87933), *E. faecium* W54 (TDC_{EFM}, accession: MH358385; $^{P}TDC_{EFM}$, accession: MH358384) were amplified using Phusion High-fidelity DNA polymerase and primers listed in **Table S7**. All amplified genes were cloned in pET15b, resulting in pSK18, pSK11, and pSK22, respectively (**Table S7**). Plasmids were maintained in *E. coli* DH5α and verified by Sanger sequencing before transformation to *E. coli* BL21 (DE3). Overnight cultures were diluted 1:50 in fresh LB medium with the appropriate antibiotic and grown to OD_{600} = 0.7-0.8. Protein translation was induced with 1mM Isopropyl β-D-1-thiogalactopyranoside (IPTG, 11411446001, Roche Diagnostics) and cultures were incubated

overnight at 18°C. Cells were washed with 1/5th of 1× ice-cold PBS and stored at −80 °C or directly used for protein isolation. Cell pellets were thawed on ice and resuspended in 1/50th of buffer A (300 mM NaCl; 10 mM imidazole; 50 mM KPO4, pH 7.5) containing 0.2 mg/mL lysozyme (105281, Merck) and 2 µg/mL DNAse (11284932001, Roche Diagnostics), and incubated for at least 10 minutes on ice before sonication (10 cycles of 15s with 30s cooling at 8 microns amplitude) using Soniprep-150 plus (Beun de Ronde, Abcoude, The Netherlands). Cell debris were removed by centrifugation at 20000 × *g* for 20 min at 4°C. The 6×his-tagged proteins were purified using a nickel-nitrilotriacetic acid (Ni-NTA) agarose matrix (30250, Qiagen). Cell-free extracts were loaded on 0.5 ml Ni-NTA matrixes and incubated on a roller shaker for 2 hours at 4°C. The Ni-NTA matrix was washed three times with 1.5 ml buffer B (300 mM NaCl; 20 mM imidazole; 50 mM KPO4, pH 7.5) before elution with buffer C (300 mM NaCl; 250 mM imidazole; 50 mM KPO4, pH 7.5). Imidazole was removed from purified protein fractions using Amicon Ultra centrifugal filters (UFC505024, Merck) and washed three times and reconstituted in buffer D (50 mM Tris-HCL; 300 mM NaCl; pH 7.5) for TDC_{EFS}, and $TDC_{EFM,}$ buffer E (100 mM KPO4; pH 7.4) for $^{P}TDC_{EFM}$ and buffer F (100 mM KPO4; 0.1 mM pyridoxal-5-phosphate; pH 7.4) for DDC. Protein concentrations were measured spectrophotometrically (Nanodrop 2000, Isogen, De Meern, The Netherlands) using the predicted extinction coefficient and molecular weight from ExPASy ProtParam tool (www.web.expasy.org/protparam/).

Enzyme kinetics and IC50 curves

Enzyme kinetics were performed in 200 mM potassium acetate buffer at pH 5 for TDC_{EFS} and TDC_{EFM}, and pH 4.5 for $^{P}TDC_{EFM}$ containing 0.1 mM PLP (pyridoxal-5-phosphate, P9255, Sigma) and 10 nM of enzyme. Reactions were performed in triplicate using L-DOPA substrate ranges from 0.5-12.5 mM and tyrosine substrate ranges from 0.25-2.5 mM. Michaelis-Menten kinetic curves were fitted using GraphPad Prism 7. The human dopa decarboxylase kinetic reactions were performed in 100 mM potassium phosphate buffer at pH 7.4 containing 0.1 mM PLP and 10 nM enzyme concentrations with L-DOPA substrate ranges from 0.1-1.0 mM. Reactions were stopped with 0.7% $HClO_4$, filtered and analyzed on the HPLC-ED-system described below. For IC50 curves, the reaction was performed using L-DOPA as the substrate at concentrations lower or equal to the Km (DDC, 0.1

mM; TDC_{EFS} and TDC_{EFM}, 1.0 mM; $^{P}TDC_{EFM}$, 0.5 mM) of the decarboxylases with 10 different concentrations of carbidopa in triplicate (human dopa decarboxylase, 0.005-2.56 µM; bacterial tyrosine decarboxylases, 2-1024 µM).

HPLC-ED analysis and sample preparation

1 mL of ice-cold methanol was added to 0.25 mL cell suspensions. Cells and protein precipitates were removed by centrifugation at 20000 × *g* for 10 min at 4°C. Supernatant was transferred to a new tube and the methanol fraction was evaporated in a Savant speed-vacuum dryer (SPD131, Fisher Scientific, Landsmeer, The Netherlands) at 60°C for 1h and 15 min. The aqueous fraction was reconstituted to 1 mL with 0.7% $HClO_4$. Samples were filtered and injected into the HPLC system (Jasco AS2059 plus autosampler, Jasco Benelux, Utrecht, The Netherlands; Knauer K-1001 pump, Separations, H. I. Ambacht, The Netherlands; Dionex ED40 electrochemical detector, Dionex, Sunnyvale, USA, with a glassy carbon working electrode (DC amperometry at 1.0 V or 0.8 V, with Ag/AgCl as reference electrode)). Samples were analyzed on a C18 column (Kinetex 5µM, C18 100 Å, 250 ×4.6 mm, Phenomenex, Utrecht, The Netherlands) using a gradient of water/methanol with 0.1% formic acid (0-10 min, 95−80% H_2O; 10-20 min, 80-5% H_2O; 20-23 min 5% H_2O; 23-31 min 95% H_2O). Data recording and analysis was performed using Chromeleon (version 6.8 SR13).

Bioinformatics

TDC_{EFS} (NCBI accession: EOT87933) was BLASTed against the protein sequences from the NIH HMP using search limits for Entrez Query "43021[BioProject]". All BLASTp hits were converted to a distance tree using NCBI TreeView (Parameters: Fast Minimum Evolution; Max Seq Difference, 0.9; Distance, Grishin). The tree was exported in Newick format and visualized in iTOL phylogentic display tool (http://itol.embl.de/). Whole genomes, or contigs containing the TDC gene cluster were extracted from NCBI and aligned using Mauve multiple genome alignment tool (v 2.4.0, www.darlinglab.org/mauve/mauve.html).

Fecal samples from patients with Parkinson's disease

Fecal samples from patients diagnosed with Parkinson's disease (n=10) on variable doses (300-1100mg L-DOPA per day) of L-DOPA/carbidopa treatment were acquired from the Movement Disorder Center at Rush University Medical Center, Chicago, Illinois, USA. Patients' characteristics

were published previously (*30*) (more details are provided in Supplementary material). Solid fecal samples were collected in a fecal bag and kept sealed in a cold environment until brought to the hospital where they were immediately stored at −80°C until analysis.

Animal experiments

Twenty-five male wild-type Groningen rats ((*31*); Groningen breed, male, age 18-24 weeks) living with 4-5 animals/cage had *ad libitum* access to water and food (RMH-B, AB Diets; Woerden, the Netherlands) in a temperature (21 ± 1°C) and humidity-controlled room (45–60% relative humidity), with a 12 hr light/dark cycle (lights off at 13:00 p.m.). On ten occasions over a period of three weeks, rats were taken from their social housing cage between CT16 and CT16.5, and put in an individual training cage (L×W×H = 25×25×40 cm) with a layer of their own sawdust without food and water. Ten minutes after transfer to these cages, rats were offered a drinking pipet in their cages with a 2.5 ml saccharine-solution (1.5 g/L, 12476, Sigma). Over the course of training, all rats learned to drink the saccharine-solution avidly. On the 11th occasion, the saccharine solution was used as vehicle for the L-DOPA/carbidopa mixture (15/3.75 mg/kg), which all rats drank within 15 seconds. Fifteen minutes after drinking the latter mixture (maximum bioavailability time point of L-DOPA in blood as previously described (*18*)), the rats were anesthetized with isoflurane and sacrificed. Blood was withdrawn by heart puncture and placed in tubes pre-coated with 5 mM EDTA. The collected blood samples were centrifuged at 1500 x g for 10 minutes at 4°C and the plasma was stored at −80°C prior to L-DOPA, dopamine, and DOPAC extraction. Luminal contents were harvested from the jejunum by gentle pressing and were snap frozen in liquid N_2, stored at −80°C until used for qPCR, and extracted of L-DOPA and its metabolites. Oral administration (drinking) of L-DOPA was corrected for by using carbidopa as an internal standard. Further, 5 rats were administered a saccharine only solution (vehicle) to check for basal levels of L-DOPA, dopamine, and DOPAC levels or background HPLC-peaks, and were also employed in jejunal content *ex vivo* incubations.

Incubation experiments of jejunal content

Luminal contents from the jejunum of wild-type Groningen rats (n=5) (see animal experiment above) were suspended in EBB (5% w/v) containing 1 mM L-DOPA and incubated for 24 hours in an anaerobic chamber at 37 °C prior to HPLC-ED analysis (DC amperometry at 0.8 V).

DNA extraction

DNA was extracted from fecal samples of Parkinson's patients and jejunal contents of rats using QIAGEN (Cat no. 51504) kit-based DNA isolation as previously described (*32*) with the following modifications: fecal samples were suspended in 1 mL inhibitEX buffer (1:5 w/v) and transferred to screw-caped tubes containing 0.5 g 0.1 mm glass beads and three 3 mm glass beads. Samples were homogenized 3 × 30 sec with 1-minute intervals on ice in a mini bead-beater (Biospec, Bartlesville, USA) 3 times.

Quantification of bacterial tyrosine decarboxylase

To cover all potential bacterial species carrying the tyrosine decarboxylase gene, a broad range of tyrosine decarboxylase genes from various bacterial genera were targeted as previously described (*33*) (**Fig. S5**). Quantitative PCR (qPCR) of tyrosine decarboxylase genes was performed on DNA extracted from each fecal sample of Parkinson's patients and rats' jejunal content using primers targeting a 350bp region of the tyrosine decarboxylase gene (Dec5f and Dec3r). Primers targeting 16sRNA gene for all bacteria (Eub338 and Eub518) were used as an internal control (**Table S7**). All qPCR experiments were performed in a Bio-Rad CFX96 RT-PCR system (Bio-Rad Laboratories, Veenendaal, The Netherlands) with iQ SYBR Green Supermix (170-8882, Bio-Rad) in triplicate on 20 ng DNA in 10 uL reactions using the manufacturer's protocol. qPCR was performed using the following parameters: 3 min at 95°C; 15 sec at 95°C, 1 min at 58°C, 40 cycles. A melting curve was determined at the end of each run to verify the specificity of the PCR amplicons. Data analysis was performed using the BioRad software. Ct[DEC] values were corrected with the internal control (Ct[16s]) and linearized using 2^-(Ct[DEC]-Ct[16s]) based on the 2^-ΔΔCt method (*34*).

Jejunal and plasma extraction of L-DOPA and its metabolites

L-DOPA, dopamine, and DOPAC were extracted from each luminal content of jejunal and plasma samples of rats using activated alumina powder (199966, Sigma) as previously described (*35*) with a few modifications. 50-200 µl blood plasma was used with 50-200 µL 1µM DHBA (3, 4-dihydroxybenzylamine hydrobromide, 858781, Sigma) as an internal standard. For jejunal luminal content samples, an equal amount of water was added (w/v), and suspensions were vigorously mixed

using a vortex. Suspensions were subsequently centrifuged at 20000 × *g* for 10 min at 4°C. 50-200 µL supernatant was used for extraction. Samples were adjusted to pH 8.6 with 200−800µl TE buffer (2.5% EDTA; 1.5 M Tris/HCl pH 8.6) and 5-10 mg of alumina was added. Tubes were mixed on a roller shaker at room temperature for 15 min and were thereafter centrifuged for 30s at 20000 × *g* and washed twice with 1 mL of H_2O by aspiration. L-DOPA and its metabolites were eluted using 0.7% $HClO_4$ and filtered before injection into the HPLC-ED-system as described above (DC amperometry at 0.8 V).

Statistics and (non)linear regression models

All statistical tests and (non)linear regression models were performed using GraphPad Prism 7. Statistical tests performed are unpaired T-tests, 2-way-ANOVA followed by a Fisher's LSD test. Specific tests and significance are indicated in the figure legends.

Supplementary Materials

Material and Methods

Fig S1. Higher L-DOPA plasma levels in germ-free mice compared to specific pathogen-free mice.

Fig S2. Microbiota harboring other PLP-dependent amino acid decarboxylases do not decarboxylate L-DOPA.

Fig S3. IC50 determination for human DOPA decarboxylase and bacterial tyrosine decarboxylases.

Fig S4. Human DOPA decarboxylase inhibitors are ineffective against the decarboxylase activity of live Enterococci.

Fig S5. Primers (Dec5f and Dec3r) targeting *Enterococcus faecalis* v583 tyrosine decarboxylase gene.

Table S1. Healthy and clinical isolates of *Enterococcus* species.

Table S2. List of microbiota harboring other PLP-dependent amino acid decarboxylases tested in this study.

Table S3. IC50 curve parameters.

Table S4. Sample information, Parkinson's patients.

Table S5. Bacterial strains and plasmids used in this study.

Table S6. Constituents of enriched beef broth (EBB) medium used in this study.

Table S7. Primer sequences used in this study.

Data file S1. Identification of conserved tyrosine decarboxylase paralogue protein ($^{P}TDC_{EFM}$) in all *E. faecium* strains analyzed.

References

1. C. T. Kahrstrom, N. Pariente, U. Weiss, Intestinal microbiota in health and disease. *Nature* **535**, 47 (2016).
2. J. M. Yano, K. Yu, G. P. Donaldson, G. G. Shastri, P. Ann, L. Ma, C. R. Nagler, R. F. Ismagilov, S. K. Mazmanian, E. Y. Hsiao, Indigenous bacteria from the gut microbiota regulate host serotonin biosynthesis. *Cell* **161**, 264-276 (2015).
3. K. Mao, A. P. Baptista, S. Tamoutounour, L. Zhuang, N. Bouladoux, A. J. Martins, Y. Huang, M. Y. Gerner, Y. Belkaid, R. N. Germain, Innate and adaptive lymphocytes sequentially shape the gut microbiota and lipid metabolism. *Nature* **554**, 255-259 (2018).
4. M. M. Pusceddu, S. El Aidy, F. Crispie, O. O'Sullivan, P. Cotter, C. Stanton, P. Kelly, J. F. Cryan, T. G. Dinan, N-3 Polyunsaturated Fatty Acids (PUFAs) Reverse the Impact of Early-Life Stress on the Gut Microbiota. *PloS one* **10**, e0139721 (2015).
5. S. El Aidy, P. van Baarlen, M. Derrien, D. J. Lindenbergh-Kortleve, G. Hooiveld, F. Levenez, J. Dore, J. Dekker, J. N. Samsom, E. E. Nieuwenhuis, M. Kleerebezem, Temporal and spatial interplay of microbiota and intestinal mucosa drive establishment of immune homeostasis in conventionalized mice. *Mucosal Immunol* **5**, 567-579 (2012).
6. J. R. Kelly, Y. Borre, O. B. C, E. Patterson, S. El Aidy, J. Deane, P. J. Kennedy, S. Beers, K. Scott, G. Moloney, A. E. Hoban, L. Scott, P. Fitzgerald, P. Ross, C. Stanton, G. Clarke, J. F. Cryan, T. G. Dinan, Transferring the blues: Depression-associated gut microbiota induces neurobehavioural changes in the rat. *Journal of psychiatric research* **82**, 109-118 (2016).
7. E. F. Enright, C. G. Gahan, S. A. Joyce, B. T. Griffin, The Impact of the Gut Microbiota on Drug Metabolism and Clinical Outcome. *The Yale journal of biology and medicine* **89**, 375-382 (2016).
8. M. Niehues, A. Hensel, In-vitro interaction of L-dopa with bacterial adhesins of Helicobacter pylori: an explanation for clinicial differences in bioavailability? *The Journal of pharmacy and pharmacology* **61**, 1303-1307 (2009).
9. P. A. B. Pereira, V. T. E. Aho, L. Paulin, E. Pekkonen, P. Auvinen, F. Scheperjans, Oral and nasal microbiota in Parkinson's disease. *Parkinsonism & related disorders* **38**, 61-67 (2017).
10. T. R. Sampson, J. W. Debelius, T. Thron, S. Janssen, G. G. Shastri, Z. E. Ilhan, C. Challis, C. E. Schretter, S. Rocha, V. Gradinaru, M. F. Chesselet, A. Keshavarzian, K. M. Shannon, R. Krajmalnik-Brown, P. Wittung-Stafshede, R. Knight, S. K. Mazmanian, Gut Microbiota Regulate Motor Deficits and Neuroinflammation in a Model of Parkinson's Disease. *Cell* **167**, 1469-1480.e1412 (2016).
11. F. Scheperjans, P. A. B. Aho V Fau - Pereira, K. Pereira Pa Fau - Koskinen, L. Koskinen K Fau - Paulin, E. Paulin L Fau - Pekkonen, E. Pekkonen E Fau - Haapaniemi, S. Haapaniemi E Fau - Kaakkola, J. Kaakkola S Fau - Eerola-Rautio, M. Eerola-Rautio J Fau - Pohja, E. Pohja M Fau - Kinnunen, K. Kinnunen E Fau - Murros, P. Murros K Fau - Auvinen, P. Auvinen, Gut microbiota are related to Parkinson's disease and clinical phenotype.
12. F. Scheperjans, V. Aho, P. A. Pereira, K. Koskinen, L. Paulin, E. Pekkonen, E. Haapaniemi, S. Kaakkola, J. Eerola-Rautio, M. Pohja, E. Kinnunen, K. Murros, P. Auvinen, Gut microbiota are related to Parkinson's disease and clinical phenotype. *Movement disorders : official journal of the Movement Disorder Society* **30**, 350-358 (2015).
13. R. Katzenschlager, A. J. Lees, Treatment of Parkinson's disease: levodopa as the first choice. *Journal of neurology* **249 Suppl 2**, Ii19-24 (2002).

14. M. Perez, M. Calles-Enriquez, I. Nes, M. C. Martin, M. Fernandez, V. Ladero, M. A. Alvarez, Tyramine biosynthesis is transcriptionally induced at low pH and improves the fitness of Enterococcus faecalis in acidic environments. *Applied microbiology and biotechnology* **99**, 3547-3558 (2015).
15. H. Zhu, G. Xu, K. Zhang, X. Kong, R. Han, J. Zhou, Y. Ni, Crystal structure of tyrosine decarboxylase and identification of key residues involved in conformational swing and substrate binding. *Scientific reports* **6**, 27779 (2016).
16. K. Zhang, Y. Ni, Tyrosine decarboxylase from Lactobacillus brevis: soluble expression and characterization. *Protein expression and purification* **94**, 33-39 (2014).
17. B. B. Williams, A. H. Van Benschoten, P. Cimermancic, M. S. Donia, M. Zimmermann, M. Taketani, A. Ishihara, P. C. Kashyap, J. S. Fraser, M. A. Fischbach, Discovery and characterization of gut microbiota decarboxylases that can produce the neurotransmitter tryptamine. *Cell host & microbe* **16**, 495-503 (2014).
18. E. Bredberg, H. Lennernäs, L. Paalzow, Pharmacokinetics of Levodopa and Carbidopa in Rats Following Different Routes of Administration. *Pharmaceutical Research* **11**, 549-555 (1994).
19. C. L. Tomlinson, R. Stowe, S. Patel, C. Rick, R. Gray, C. E. Clarke, Systematic review of levodopa dose equivalency reporting in Parkinson's disease. *Movement disorders : official journal of the Movement Disorder Society* **25**, 2649-2653 (2010).
20. C. Pellegrini, L. Antonioli, R. Colucci, V. Ballabeni, E. Barocelli, N. Bernardini, C. Blandizzi, M. Fornai, Gastric motor dysfunctions in Parkinson's disease: Current pre-clinical evidence. *Parkinsonism & related disorders* **21**, 1407-1414 (2015).
21. J. E. Richter, The many manifestations of gastroesophageal reflux disease: presentation, evaluation, and treatment. *Gastroenterology clinics of North America* **36**, 577-599, viii-ix (2007).
22. A. H. Tan, S. Mahadeva, A. M. Thalha, P. R. Gibson, C. K. Kiew, C. M. Yeat, S. W. Ng, S. P. Ang, S. K. Chow, C. T. Tan, H. S. Yong, C. Marras, S. H. Fox, S. Y. Lim, Small intestinal bacterial overgrowth in Parkinson's disease. *Parkinsonism & related disorders* **20**, 535-540 (2014).
23. R. Pfeiffer, Beyond here be dragons: SIBO in Parkinson's disease. *Movement disorders : official journal of the Movement Disorder Society* **28**, 1764-1765 (2013).
24. E. G. Zoetendal, J. Raes, B. van den Bogert, M. Arumugam, C. C. Booijink, F. J. Troost, P. Bork, M. Wels, W. M. de Vos, M. Kleerebezem, The human small intestinal microbiota is driven by rapid uptake and conversion of simple carbohydrates. *The ISME journal* **6**, 1415-1426 (2012).
25. S. El Aidy, B. van den Bogert, M. Kleerebezem, The small intestine microbiota, nutritional modulation and relevance for health. *Curr Opin Biotechnol* **32c**, 14-20 (2014).
26. D. E. Freedberg, N. C. Toussaint, S. P. Chen, A. J. Ratner, S. Whittier, T. C. Wang, H. H. Wang, J. A. Abrams, Proton Pump Inhibitors Alter Specific Taxa in the Human Gastrointestinal Microbiome: A Crossover Trial. *Gastroenterology* **149**, 883-885.e889 (2015).
27. J. E. Valenzuela, C. P. Dooley, Dopamine antagonists in the upper gastrointestinal tract. *Scandinavian journal of gastroenterology. Supplement* **96**, 127-136 (1984).
28. P. A. Kempster, D. R. Williams, M. Selikhova, J. Holton, T. Revesz, A. J. Lees, Patterns of levodopa response in Parkinson's disease: a clinico-pathological study. *Brain* **130**, 2123-2128 (2007).
29. J. M. Auchtung, C. D. Robinson, R. A. Britton, Cultivation of stable, reproducible microbial communities from different fecal donors using minibioreactor arrays (MBRAs). *Microbiome* **3**, 42 (2015).
30. A. Keshavarzian, S. J. Green, P. A. Engen, R. M. Voigt, A. Naqib, C. B. Forsyth, E. Mutlu, K. M. Shannon, Colonic bacterial composition in Parkinson's disease. *Movement disorders : official journal of the Movement Disorder Society* **30**, 1351-1360 (2015).
31. J. M. Koolhaas, C. M. Coppens, S. F. de Boer, B. Buwalda, P. Meerlo, P. J. A. Timmermans, The Resident-intruder Paradigm: A Standardized Test for Aggression, Violence and Social Stress. *Journal of Visualized Experiments : JoVE*, 4367 (2013).

32. E. G. Zoetendal, H. G. Heilig, E. S. Klaassens, C. C. Booijink, M. Kleerebezem, H. Smidt, W. M. de Vos, Isolation of DNA from bacterial samples of the human gastrointestinal tract. *Nature protocols* **1**, 870-873 (2006).
33. S. Torriani, V. Gatto, S. Sembeni, R. Tofalo, G. Suzzi, N. Belletti, F. Gardini, S. Bover-Cid, Rapid detection and quantification of tyrosine decarboxylase gene (tdc) and its expression in gram-positive bacteria associated with fermented foods using PCR-based methods. *Journal of food protection* **71**, 93-101 (2008).
34. K. J. Livak, T. D. Schmittgen, Analysis of relative gene expression data using real-time quantitative PCR and the 2(-Delta Delta C(T)) Method. *Methods (San Diego, Calif.)* **25**, 402-408 (2001).
35. M. F. Ganhao, J. Hattingh, M. L. Hurwitz, N. I. Pitts, Evaluation of a simple plasma catecholamine extraction procedure prior to high-performance liquid chromatography and electrochemical detection. *Journal of chromatography* **564**, 55-66 (1991).

Acknowledgements

We thank Dr. Saskia van Hemert and Dr. Coline Gerritsen of Winclove Probiotics, Amsterdam, Netherlands, for providing us *E.faecium* W54 and *L.brevis* W63, as well as their sequencing data; Dr. Jan Kok of Department of Molecular genetics, University of Groningen, Netherlands, and Dr. Miguel A. Alvarez of Instituto de Productos Lácteos de Asturias, Villaviciosa, Spain for providing the mutant strain *E. faecalis* v583; Dr. Uwe Tietge and Rema H. Mistry, MSc. of the Department of Pediatrics, University Medical Centre Groningen, Groningen, Netherlands for providing assistance with germ-free and specific pathogen free mice; and Dr. Phillip A. Engen, Division of Digestive Disease and Nutrition, Section of Gastroenterology, Rush University Medical Center, USA for assisting in preparing fecal specimen from Parkinson's patients for shipment.

Funding: SEA is supported by a Rosalind Franklin Fellowship, co-funded by the European Union and University of Groningen, The Netherlands.

Authors Contributions: S.P.K. and S.E.A conceived and designed the study. S.P.K, A.K.F., A.O.E.G., M.C., A.K., G.D., S.E.A performed the experiments and S.P.K and S.E.A analyzed the data. S.P.K and S.E.A. wrote the original manuscript that was reviewed by A.K.F., S.E.A., A.K., G.D. Funding was acquired by S.E.A.

Conflict of interest: The authors declare no conflicts of interest.

Figures, Tables, and legends

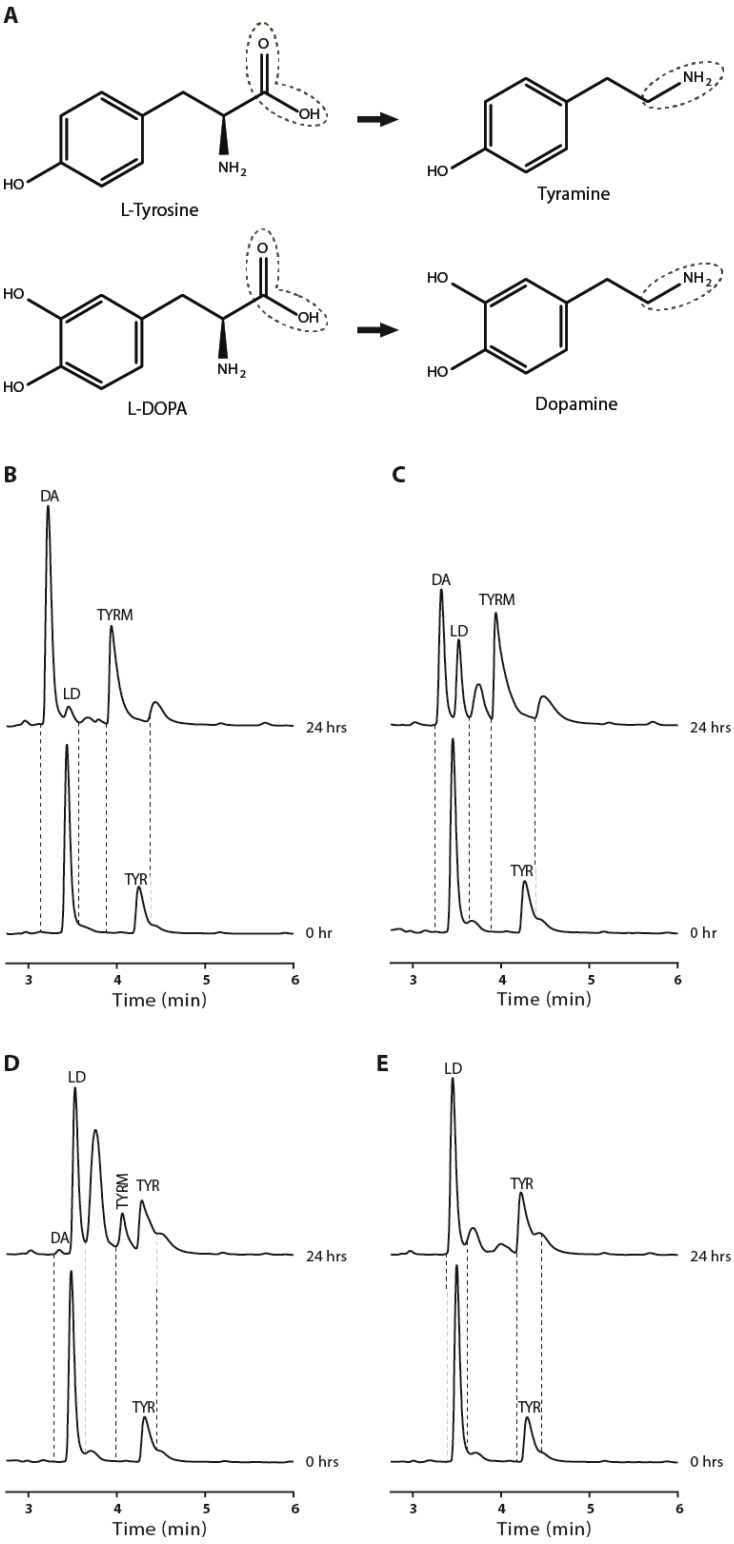

Fig. 1. Jejunal bacteria decarboxylate L-DOPA to dopamine in alignment with their production of tyramine *ex vivo*. (**A**) Decarboxylation reaction for tyrosine and L-DOPA. (**B, C**) Bacterial conversion of tyrosine (TYR) to tyramine (TYRM) and 1 mM of supplemented L-DOPA (LD) to

573 dopamine (DA), during 24 hrs of incubation. (**D**) Detection of low amounts of dopamine production
574 when tyrosine was still abundant and tyramine production was relatively low. (**E**) No tyrosine was
575 converted to tyramine, accordingly no L-DOPA was converted to dopamine.

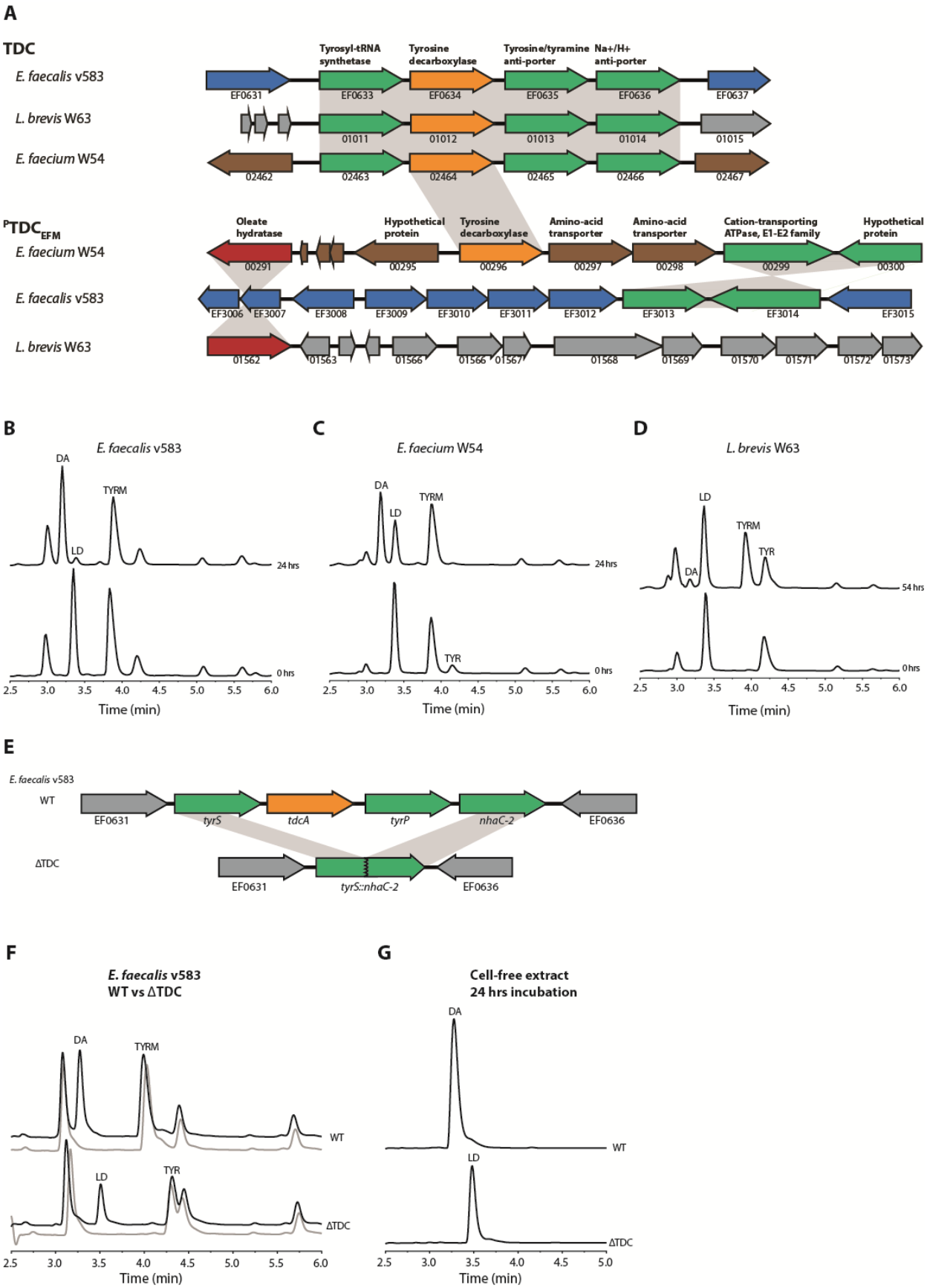

Fig. 2. Gut bacteria harboring tyrosine decarboxylases are responsible for L-DOPA decarboxylation. (**A**) Aligned genomes of *E. faecium*, *E. faecalis*, and *L. brevis.* The conserved *tdc*-

operon is depicted with *tdc*-gene in orange. Overnight cultures of (**B**) *E. faecalis* v583, (**C**) *E. faecium* W54, and (**D**) *L. brevis* W63 incubated anaerobically at 37 °C with 100 µM of L-DOPA (LD). (**E**) Genomic scheme showing the differences between EFS^{WT} (this study) and $EFS^{\Delta TDC}$*(14)*. (**F**) Overnight cultures of EFS^{WT} and $EFS^{\Delta TDC}$ incubated anaerobically at 37 °C with 100 uM L-DOPA (black line) compared to control (grey line) where no L-DOPA was added. (**G**) Comparison of enzyme activity of EFS^{WT} and $EFS^{\Delta TDC}$ cell-free protein extracts after O/N incubation with 1 mM L-DOPA at 37 °C. Curves represent 3 biological replicates.

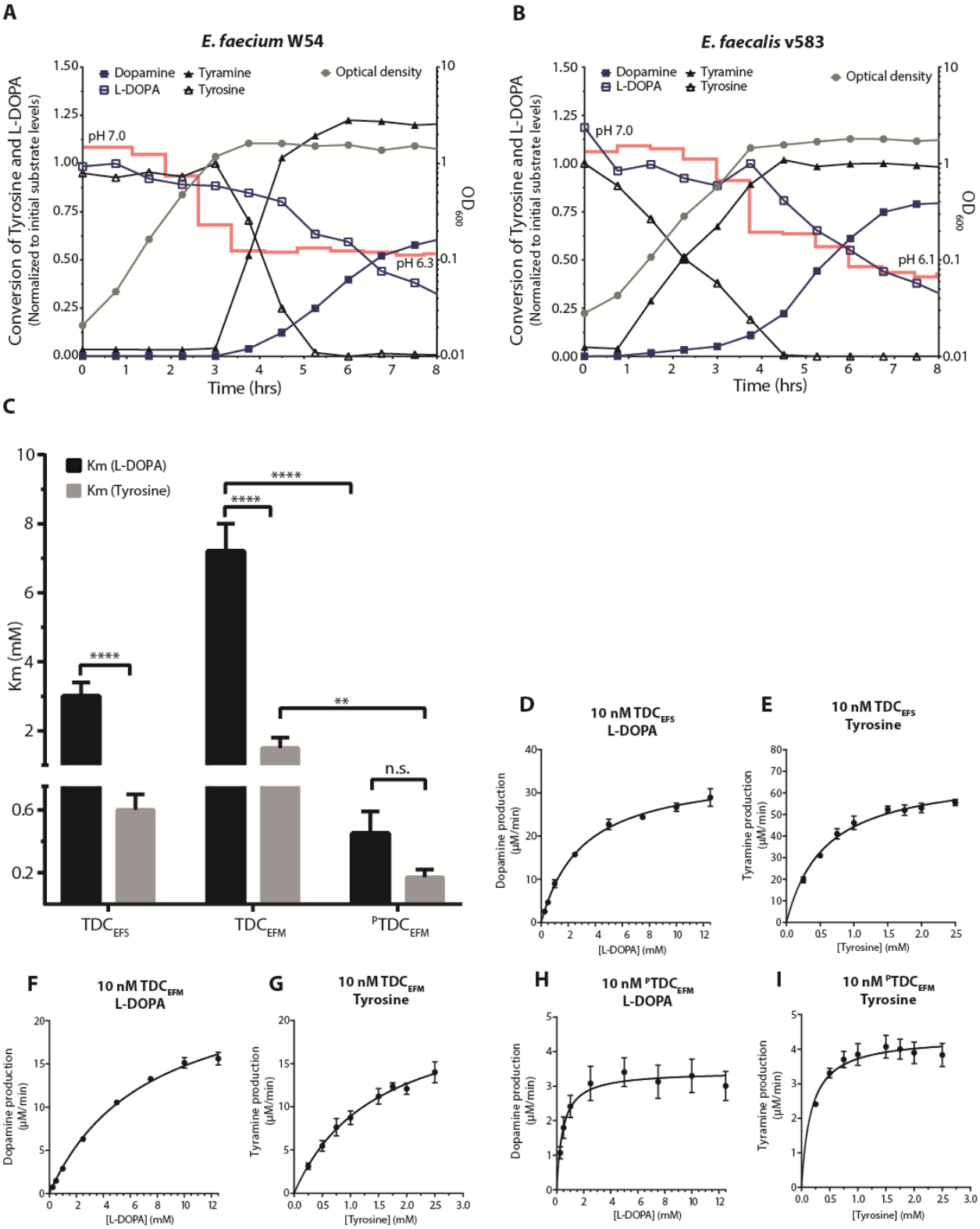

Fig. 3. Enterococci decarboxylate L-DOPA in presence of tyrosine despite higher affinity for tyrosine *in vitro*. Growth curve (grey circle, right Y-axis) of *E. faecium* W54 (**A**) and *E. faecalis* (**B**) plotted together with L-DOPA (open square), dopamine (closed square), tyrosine (open triangle), and tyramine (closed triangle) levels (left Y-axis). Concentrations of product and substrate were

592 normalized to the initial levels of the corresponding substrate. pH of the culture is indicated over time
593 as a red line. (**C**) Substrate affinity (Km) for L-DOPA and tyrosine for purified tyrosine
594 decarboxylases from *E. faecalis* v583 (TDC_{EFS}), *E. faecium* W54 (TDC_{EFM}, $^{P}TDC_{EFM}$). (**D-I**)
595 Michaelis-Menten kinetic curves for L-DOPA and tyrosine as substrate for TDC_{EFS} (**D,E**), TDC_{EFM}
596 (**F,G**), and $^{P}TDC_{EFM}$ (**H,I**). Reactions were performed in triplicate using L-DOPA concentrations
597 ranging from 0.5-12.5 mM and tyrosine concentrations ranging from 0.25-2.5 mM. The enzyme
598 kinetic parameters were calculated using nonlinear Michaelis-Menten nonlinear regression model.
599 Significance was tested using 2-way-Anova, Fisher LSD test, (*=p<0.02 **=p<0.01 ****<0.0001).
600

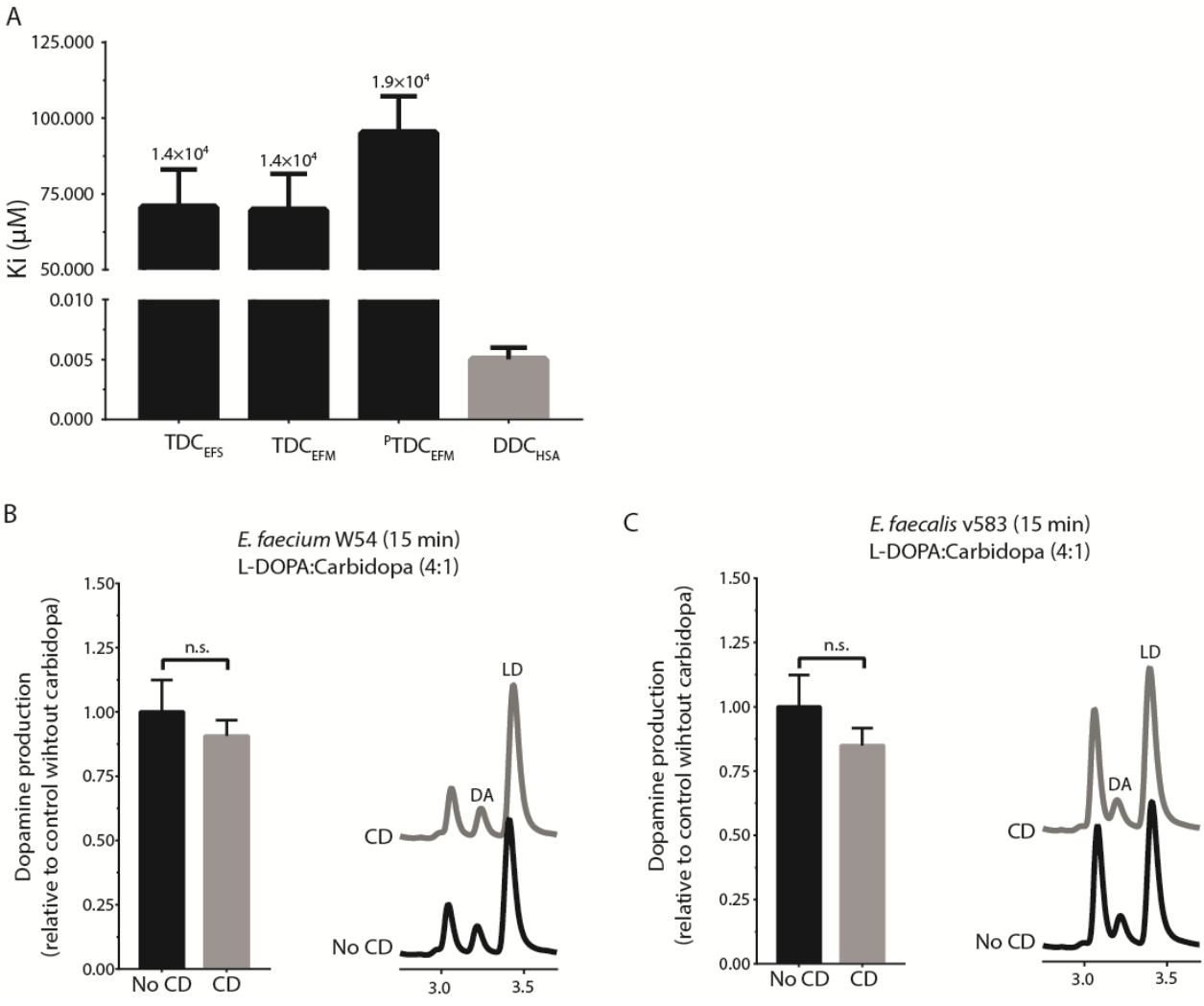

Fig. 4. Human DOPA decarboxylase inhibitor, carbidopa, does not inhibit bacterial decarboxylation. (**A**) Inhibitory constants (Ki) of bacterial decarboxylases (black) and human DOPA decarboxylase (grey), with fold-difference between bacterial and human decarboxlyase displayed on top of the bars. Quantitative comparison of dopamine (DA) production by *E. faecium* W54, (**B**) and *E. faecalis* v583, (**C**) at stationary phase after 15 min, with representative HPLC-ED curve. Bacterial cultures (n=3) were incubated with 100 µM L-DOPA (LD) or a 4:1 mixture (in weight) of L-DOPA and carbidopa (CD) (100 µM L-DOPA and 21.7 µM carbidopa). Significance was tested using a parametric unpaired T-test.

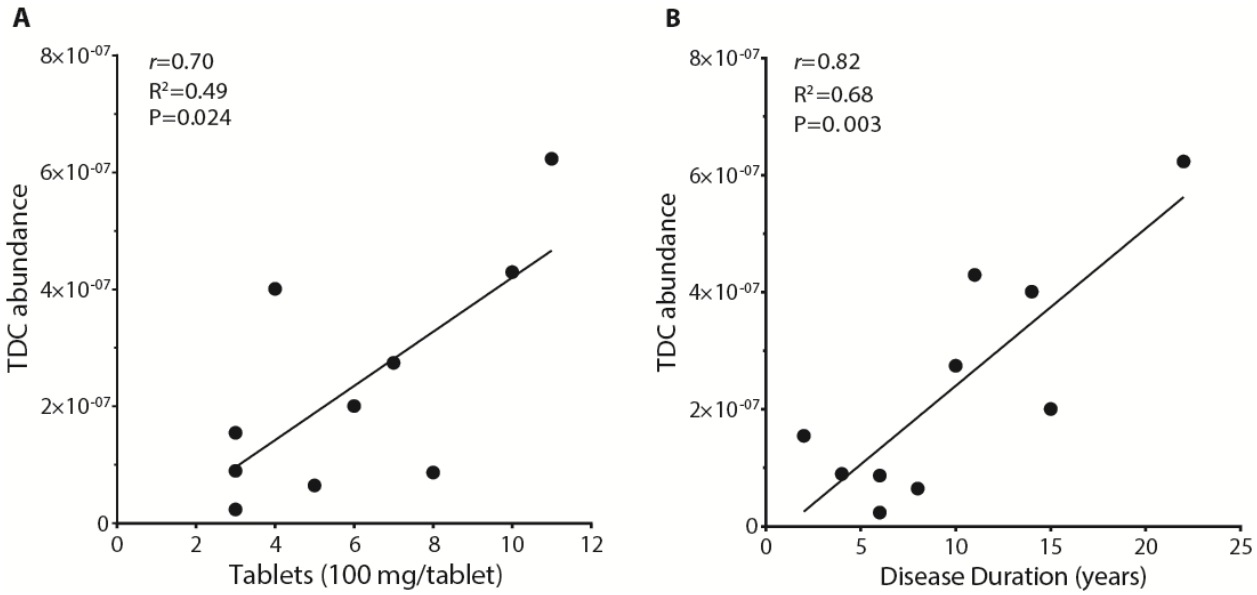

611

612 **Fig. 5. Tyrosine decarboxylase gene abundance correlates with daily L-DOPA dose and disease**
613 **duration in fecal samples of Parkinson's patients.** (**A**) Scatter plot of tyrosine decarboxylase
614 (TDC)-gene abundance measured by qPCR in fecal samples of Parkinson's patients (n=10) versus
615 daily L-DOPA dosage fitted with linear regression model. (**B**) Scatter plot of TDC gene abundance
616 from the same samples versus disease duration fitted with a linear regression model. Pearson's *r*
617 analysis was used to determine significant correlations between tyrosine decarboxylase -gene
618 abundance and dosage (r=0.70, R^2=0.49, *P value*=0.024) or disease duration (r = 0.82, R^2 = 0.68, *P*
619 *value* = 0.003).

620

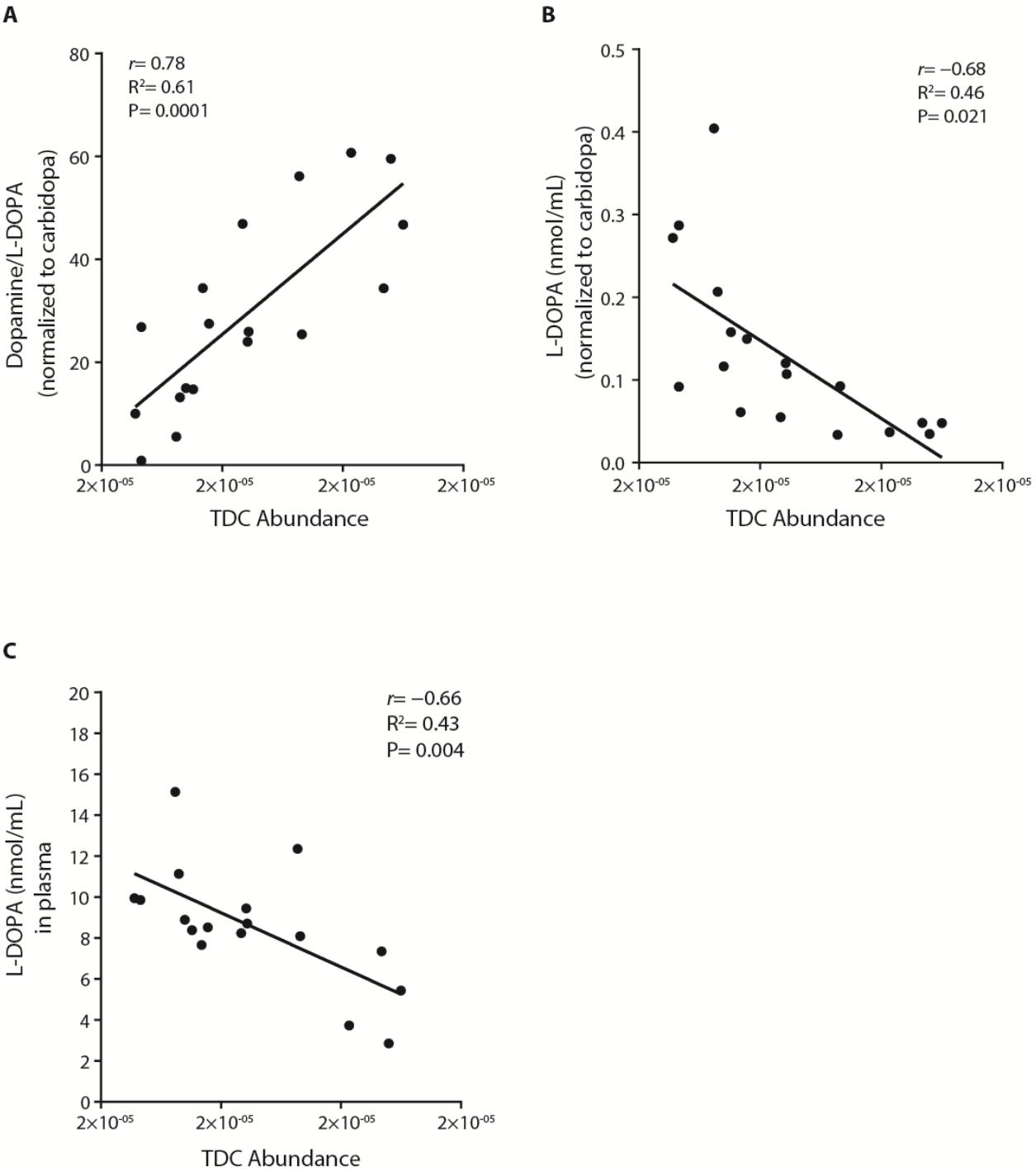

621

622 **Fig. 6**. **Tyrosine decarboxylase gene abundance correlates with L-DOPA bioavailability in rats.**
623 Scatter plot of tyrosine decarboxylase (TDC)-gene abundance measured by qPCR in jejunal content of
624 wild-type Groningen rats (n=18) orally supplied with a L-DOPA/carbidopa mixture (4:1) versus (**A**)
625 the dopamine/L-DOPA levels in the jejunal content, (**B**) the L-DOPA levels in the jejunal content, (**C**)
626 or the L-DOPA levels in the plasma, fitted with a linear regression model. Pearson's *r* correlation was
627 used to determine significant correlations between TDC-gene abundance and jejunal dopamine levels

628 (r = 0.78, R^2 = 0.61, *P* value = 0.0001), jejunal L-DOPA levels (r = −0.68, R^2 = 0.46 *P* value = 0.021),

629 or plasma L-DOPA levels (r = −0.66, R^2 = 0.43, *P* value = 0.004).

630

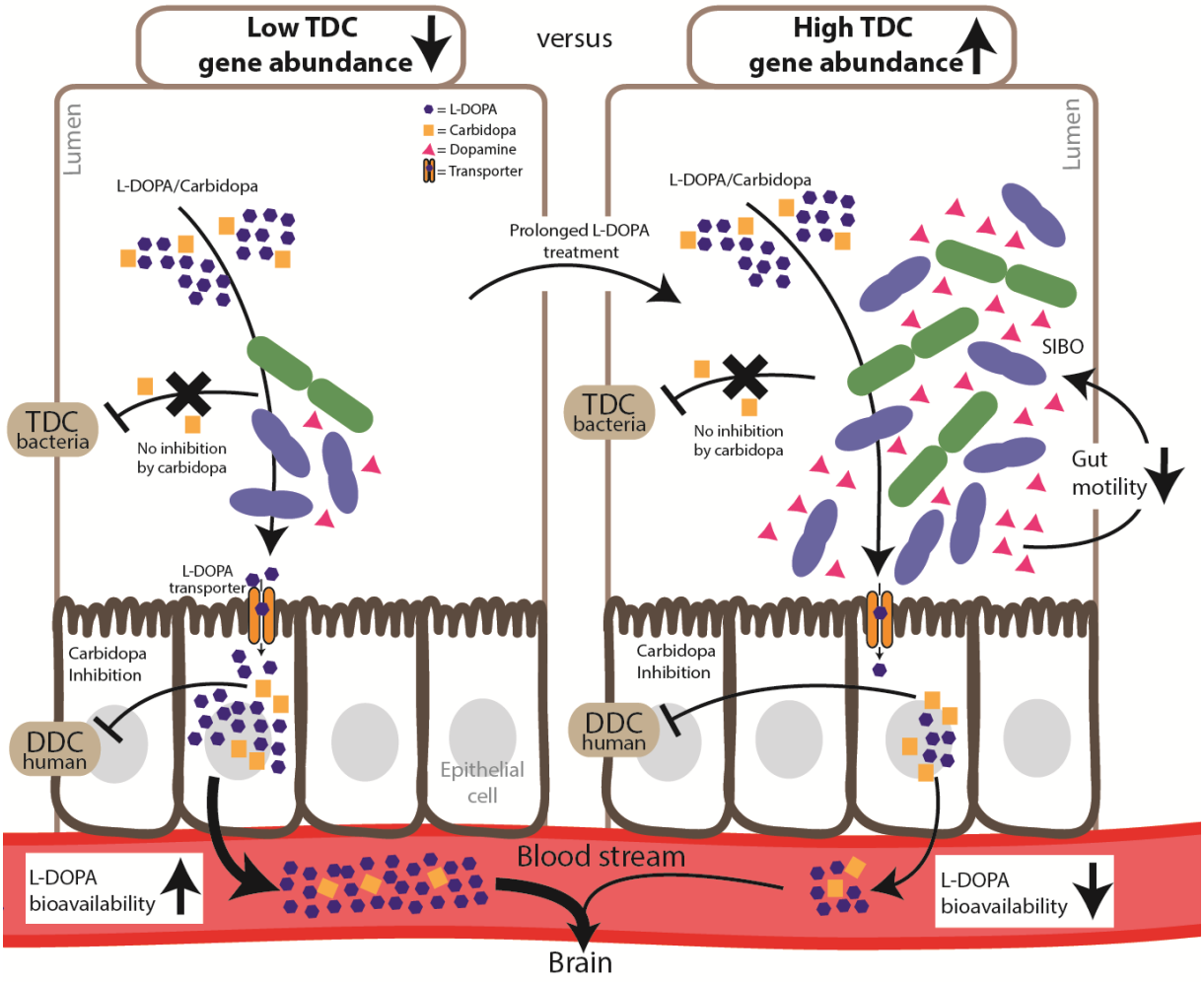

631

632 **Fig. 7. Higher abundance of tyrosine decarboxylase is cause and/or effect of fluctuating L-DOPA**
633 **responsiveness?** A model representing two opposing situations, in which the proximal small intestine
634 is colonized by low (left) or high abundance of tyrosine decaroboxylase-encoding bacteria. The latter
635 could result from or lead to increased individual L-DOPA dosage intake.

636

637

638 **Table 1. Michaelis-Menten kinetic parameters.** Enzyme kinetic parameters were determined by
639 Michaelis-Menten nonlinear regression model for L-DOPA and Tyrosine as substrates. ± indicates the
640 standard error.

L-DOPA	pH 5.0	pH 5.0	pH 4.5	pH 7.4
	TDC_{EFS}	**TDC_{EFM}**	**$^{P}TDC_{EFM}$**	**DDC**
[E] (nM)	10.00	10.00	10.00	10.00
Km (mM)	3±0.4	7.2±0.8	0.4±0.1	0.1±0.01
Vmax (µM/min)	35.3±1.4	25.5±1.3	3.4±0.2	1.4±0.03
Kcat (min-1)	3531±137	2549±133	342.4±21	136.9±3
Kcat/Km (min-1/mM-1)	1160	352	764	1567
R^2	0.978	0.990	0.621	0.962

Tyrosine	pH 5.0	pH 5.0	pH 4.5
	TDC_{EFS}	**TDC_{EFM}**	**$^{P}TDC_{EFM}$**
[E] (nM)	10.00	10.00	10.00
Km (mM)	0.6±0.1	1.5±0.3	0.2±0.05
Vmax (µM/min)	69.6±2.9	22±2.5	4.4±0.2
Kcat (min-1)	6963±288	2204±247	435.6±19.2
Kcat/Km (min-1/mM-1)	12216	1493	2558
R^2	0.928	0.902	0.589

641